Mutagenic Potential of Stereoisomeric Bay Region (+)- and (−)-*cis*-*anti*-Benzo[*a*]pyrene Diol Epoxide-N^2-2′-deoxyguanosine Adducts in *Escherichia coli* and Simian Kidney Cells†

Andrea Fernandes,‡ Tongming Liu,§ Shantu Amin,|| Nicholas E. Geacintov,§ Arthur P. Grollman,‡ and Masaaki Moriya*,‡

Department of Pharmacological Sciences, State University of New York, Stony Brook, New York 11794-8651, Department of Chemistry, New York University, New York, New York 10003, and American Health Foundation, Valhalla, New York 10595

Received February 19, 1998; Revised Manuscript Received May 20, 1998

ABSTRACT: We have investigated the mutagenic potential of site-specifically positioned DNA adducts with (+)- and (−)-cis-anti stereochemistry derived from the binding of *r*7,*t*8-dihydroxy-*t*9,10-epoxy-7,8,9,10-tetrahydrobenzo[*a*]pyrene (BPDE) to N^2-2′-deoxyguanosine (G_1 or G_2) in the sequence context $^{5'}$TCCTCCTG_1 G_2CCTCTC. BPDE-modified oligodeoxynucleotides were ligated to a single-stranded DNA vector and replicated in *Escherichia coli* or simian kidney (COS7) cells. The presence of (+)- or (−)-cis adduct strongly reduced the yield of transformants in *E. coli*, and the yield was improved by the induction of SOS functions. Both adducts were mutagenic in *E. coli* and COS cells, generating primarily G → T transversions. In *E. coli*, the (−)-cis adduct was more mutagenic than the (+)-cis adduct, while in COS cells, both adducts were equally mutagenic. These results were compared with those obtained with stereoisomeric (+)- and (−)-trans adducts [Moriya, M., et al. (1996) *Biochemistry 35*, 16646−16651). In *E. coli*, cis adducts, especially (−)-cis adducts, are consistently more mutagenic than the comparable trans adduct. In COS cells, trans adducts yield higher frequencies of mutations than the two cis adducts and, with the exception of the high-mutation frequency associated with the (+)-trans adduct at G_2, relatively small differences in mutation frequencies are observed for the three other adducts. In *E. coli*, mutation frequency is a pronounced function of adduct stereochemistry and adduct position. These findings suggest that the fidelity of translesional synthesis across BPDE-dG adducts is strongly influenced by adduct stereochemistry, nucleotide sequence context, and the DNA replication complex.

Polycyclic aromatic hydrocarbons (PAHs)[1] are ubiquitous environmental pollutants that can be activated by cellular multifunction oxidases to produce a variety of oxygenated metabolites (*1*). The diol epoxide derivatives bind covalently to cellular DNA, thus inducing mutations and initiating tumorigenesis in animal model systems (*2*). Benzo[*a*]pyrene (BP), one of the most widely studied PAH compounds (*3*), is metabolized to oxygenated derivatives, including the biologically important (+)-enantiomer of *r*7,*t*8-dihydroxy-*t*9,10-epoxy-7,8,9,10-tetrahydrobenzo[*a*]pyrene (*anti*-BPDE, or BPDE). The (+)-7*R*,8*S*,9*S*,10*R*-enantiomer [(+)-*anti*-BPDE] is more tumorigenic than the (−)-7*S*,8*R*,9*R*,10*S*-enantiomer [(−)-*anti*-BPDE] when applied to mouse skin and in the newborn mouse lung model (*4*, *5*). In mammalian cell systems, (+)-*anti*-BPDE is more mutagenic than the (−)-enantiomer (*6*−*9*), while in bacteria the relative mutagenicities of the two enantiomers depend on the test system utilized (*6*, *8*).

The tumorigenic activities of BPDE correlate with the formation of covalent adducts with cellular DNA (*10*, *11*). Both BPDE enantiomers react with native DNA by binding predominantly to the exocyclic amino group of 2′-deoxyguanosine residues (dG) by trans or cis addition of N^2-dG to the C10-position of *anti*-BPDE (*12*−*15*). While trans addition is dominant, smaller quantities of *cis*-N^2-dG as well as N^6-2′-deoxyadenosine adducts also are formed (*15*).

When cells are treated with BPDE, a variety of DNA adducts is produced. Due to the stereochemical diversity of these adducts, it is not feasible to relate the observed mutagenic spectra and mutagenic specificities to a particular type of lesion. Nevertheless, useful observations have been made in random modification experiments using racemic mixtures of *anti*-BPDE (*16*−*21*), the optically resolved (+)-*anti*-BPDE (*22*, *23*), or (−)-*anti*-BPDE enantiomers (*9*). The most frequently observed point mutations recorded in these studies were G → T transversions: G → A and G → C base substitutions also were observed, but generally were less abundant.

† This research was supported by NIH Grants ES04068 and CA17395 (to A.P.G.) and CA 20851 (to N.E.G.).

* To whom correspondence should be directed.
‡ State University of New York, Stony Brook.
§ New York University.
|| American Health Foundation.

[1] Abbreviations: BP, benzo[*a*]pyrene; BPDE, *r*7,*t*8-dihydroxy-*t*9, 10-epoxy-7,8,9,10-tetrahydrobenzo[*a*]pyrene; CD, circular dichroism; PAH, polycyclic aromatic hydrocarbons; ss, single stranded; TEAA, triethylammonium acetate.

S0006-2960(98)00401-2 CCC: $15.00
Published on Web 06/25/1998

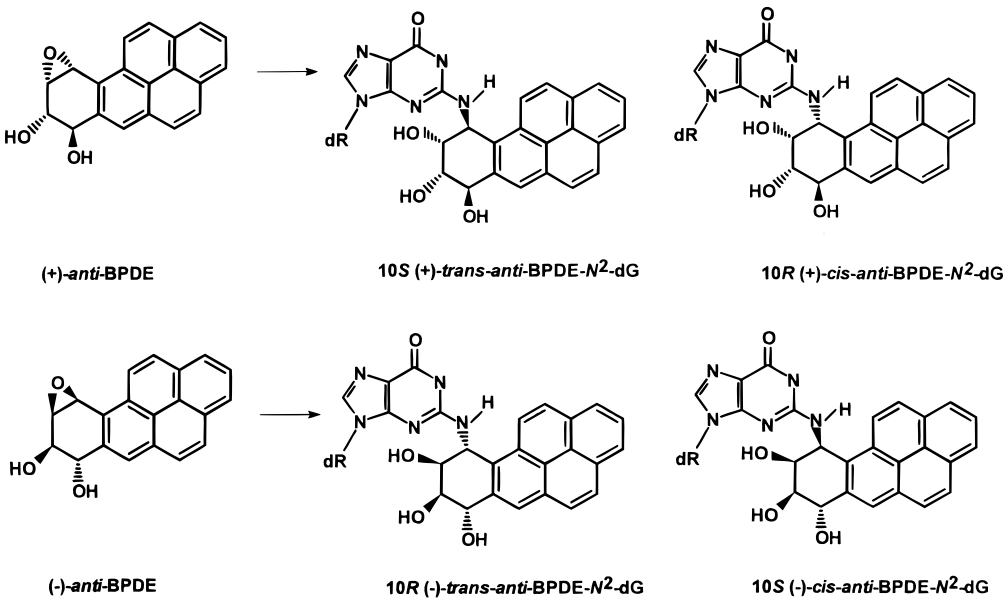

FIGURE 1: Structures of (+)- and (−)-*anti*-BPDE and stereochemical characteristics of the 10*S*-(+)-*trans*-, 10*R*-(+)-*cis*-, 10*R*-(−)-*trans*-, and 10*S*-(−)-*cis*-*anti*-BPDE-N^2-dG adducts.

Site-specific mutagenesis experiments in which a single adducted base is embedded in a defined sequence context represent an important tool for correlating adduct structure with mutagenic potential (*24*−*26*). In the early 1990s, oligonucleotides site-specifically modified with stereochemically defined BPDE-N^2-dG lesions became available. Several site-specific mutagenesis studies with BPDE adducts in cells have been published; these include investigations of *anti*-BPDE-N^2-dG adducts embedded in different sequence contexts (*27*−*33*).

In a previous study, we compared the mutagenic potentials of (+)- and (−)-*trans*-*anti*-BPDE-N^2-dG lesions positioned at G_2 or G_1 of codons 60 and 61, respectively, in the noncoding strand of the human c-Ha-*ras* 1 protooncogene (*29*):

$$\begin{array}{c} \underline{63}\ \ \underline{62}\ \ \underline{61}\ \ \underline{60} \\ 5'\text{-TC CTC CTG}_1\ \text{G}_2\text{CC TCTC} \end{array} \qquad \mathbf{I}$$

These modified sequences were incorporated into a single-stranded shuttle vector and introduced into *Escherichia coli* or simian kidney (COS7) cells. The mutation frequencies and specificities for the four site-specific DNA adducts were then analyzed. The most abundant mutations observed were G → T transversions; mutation frequencies depended strongly on the host cell, adduct stereochemistry, and position of the lesion in sequence **I**.

An important unresolved question is whether minor BPDE-DNA adducts, such as the *cis*-*anti*-BPDE-N^2-dG lesions, might contribute significantly to overall mutagenicity and/or different mutagenic specificities when cells are exposed to racemic *anti*-BPDE (*7*, *12*−*15*). If this were the case, minor BPDE-DNA adducts would assume greater significance than their relative abundance might suggest. To compare the mutational frequencies and specificities of stereoisomeric *cis* and *trans*-*anti*-BPDE-N^2-dG lesions within the same sequence context (*29*), we established the mutagenic potential of (+)- and (−)-*cis*-*anti*-BPDE-N^2-dG adducts (Figure 1) at G_1 and G_2 in sequence **I**.

MATERIALS AND METHODS

BPDE-Modified Oligonucleotides. Oligonucleotides (sequence **I**) containing (+)- or (−)-*cis*-*anti*-BPDE-N^2-dG at G_1 or G_2 were prepared as previously reported (*29*, *34*) with minor modifications in the procedure. Briefly, racemic BPDE, synthesized as described by Yagi et al. (*35*), was added to a 1.5 mM solution of oligonucleotide **I** in 50 mM triethylammonium acetate (TEAA) buffer solution (pH 7) to yield a 0.25 mM BPDE solution. The solution was incubated for 16 h at 20 °C. The 7,8,9,10-tetrahydroxytetrahydrobenzo[*a*]pyrene (tetraol) hydrolysis products were then extracted with water-saturated ether. This cycle was repeated five times to increase the overall BPDE-oligonucleotide adduct yield. BPDE-modified oligonucleotides were separated from the unmodified oligonucleotides using three separate reversed-phase HPLC steps. In the first step, a semipreparative 75 Å poly(styrene-divinylbenzene) PRP-1 column (Hamilton Co., Reno, NE) was used to separate BPDE-modified oligonucleotides into three fractions using a 15 to 90% methanol-sodium phosphate buffer (20 mM, pH 7.0) gradient in 90 min (2 mL/min). Aliquots of the three fractions were combined and subjected to reversed-phase HPLC separation using a C-18 column (10 × 250 mm) and an 11 to 14% acetonitrile-TEAA buffer (50 mM, pH 7.0) gradient (90 min, 2 mL/min). Each fraction was collected and subjected to further purification using a 4.6 × 250 mm C-18 column and a 18 to 28% 20 mM sodium phosphate buffer gradient (90 min, 1 mL/min). The stereochemical properties of the BPDE-modified oligonucleotides were determined by digesting each to the nucleoside level with snake venom phosphodiesterase and bacterial alkaline phosphatase (*34*). BPDE-modified deoxyguanosines were separated from the unmodified nucleosides using a C-18 column and 0 to 85% methanol-20 mM sodium phosphate buffer gradient eluted at a flow rate of 1 mL/min over 120 min. The stereochemical properties of the *anti*-BPDE-N^2-dG adducts in each fraction were identified by circular dichroism (CD) and by coelution techniques using (+)-*cis*-

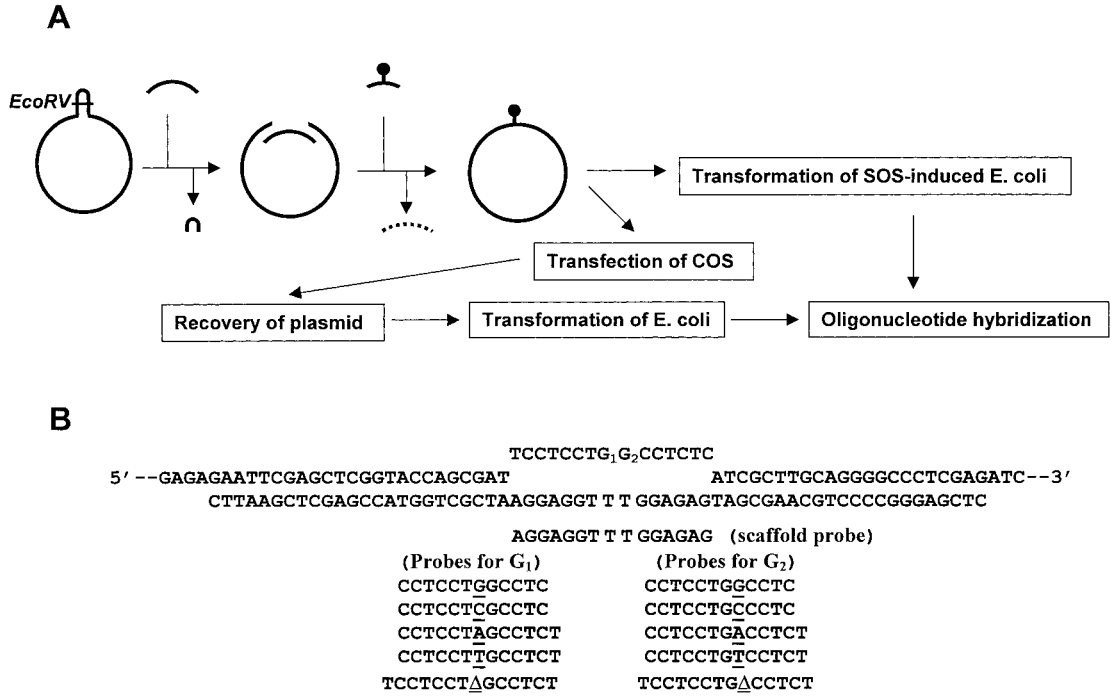

FIGURE 2: (A) Experimental procedure. See text for explanation; (B) sequences of gapped region, 61-mer scaffold, modified 15-mer and probes for mutation analysis. *cis*-BPDE-dG adduct is located at G_1 or G_2. Targeted events are determined with a set of probes for G_1 or G_2. The underlined 15-mer that contains three base mismatches to the 15-mer insert is used to detect plasmid derived from the 61-mer scaffold.

and (−)-cis-*anti*-BPDE-N^2-dG standards prepared by the methods described by Cheng et al. (*15*).

The precise site of modification, G_1 or G_2, was established by the Maxam−Gilbert method as described previously (*29*, *34*). Site-specifically modified oligonucleotides were repurified using a denaturing 20% polyacrylamide gel. Single bands were visualized by UV shadowing. The bands were cut out and the DNA extracted with TE buffer (10 mM Tris-HCl and 1 mM EDTA), followed by HPLC purification to remove salts and urea.

Construction of Modified Vectors and Mutagenesis Assays. Experimental procedure for site-specific mutagenesis has been described in detail previously (*36*−*38*) and is shown schematically in Figure 2. In brief, BPDE-modified oligodeoxynucleotides were ligated to the single-stranded (ss) shuttle vector pMS2. This vector contains the ColE1, f1, and SV40 origins of replication (*38*). Single-stranded pMS2 was prepared from JM109 harboring this plasmid with the aid of the helper phage, VCSM13 (Stratagene). ssDNA was hybridized with a 61-mer and then digested with *Eco*RV. The site for this enzyme is located in the hairpin region of ssDNA, and the linearization of ssDNA in the presence of the 61-mer creates gapped ssDNA (Figure 2A). Modified or unmodified 15-mer was hybridized to the gap and ligated to the vector with T4 DNA ligase. The hybridized 61-mer was then removed by digesting with exonuclease III and T4 DNA polymerase in the absence of dNTP. The ssDNA construct was introduced into SV40-transformed simian kidney cells (COS7) by the Lipofectin method (GIBCO/BRL). Progeny plasmid was recovered 48 h after transfection by the method of Hirt (*39*), and then used to transform *E. coli* DH10B (GIBCO/BRL) for mutational analysis. For experiments in *E. coli*, AB1157 that had been pretreated with UV at 20 J/m^2 to induce SOS functions was transformed with the DNA construct by the method of Chung et al. (*40*). Bacterial transformants of AB1157 and DH10B (the latter were obtained from COS experiments) were inoculated individually to a 96-well plate. After 6 h of incubation at 37 °C, bacterial culture was spotted onto filter paper on an agar plate containing ampicillin (100 μg/mL). The plate was incubated at 37 °C overnight. Plasmid DNA was fixed onto the filter and hybridized with one of the radioactive probes shown in Figure 2B to determine the base at the site of the DNA adduct. Progeny derived from 61-mer was detected with the probe (Figure 2B, underlined) that contained three base mismatches (TTT/TG_1G_2) to the 15-mer insert. Examples of autoradiograph of hybridization have been presented elsewhere (*41*).

RESULTS

Characterization of BPDE-Modified Oligodeoxynucleotides. The isolation and characterization of oligodeoxynucleotides with *trans-anti*-BPDE-N^2-dG lesions at G_1 or G_2 embedded in sequence **I** have been described (*29*, *34*). Similar procedures were used to purify and characterize oligodeoxynucleotides modified with *cis-anti*-BPDE-N^2-dG.

Oligonucleotides containing cis adducts were obtained in lower yields than those with trans adduct stereochemistry. Following enzymatic digestion of oligonucleotides to the nucleoside level and separation of BPDE-N^2-dG nucleoside adducts from unmodified 2′-nucleosides, CD spectra of BPDE-N^2-dG adducts were obtained as shown in Figure 3. For the two samples derived from digestion of BPDE-modified oligonucleotides, the signal/noise ratio was lower than for the (+)-cis- and (−)-*cis-anti*-BPDE-N^2-dG mononucleoside adduct standards. This is due to the fact that a minimum amount of the modified oligonucleotides was digested in order to conserve precious materials. The CD spectra of the (+)-*cis*- and (−)-*cis*-BPDE-N^2-dG adducts, derived from digestion of the modified oligonucleotides, are

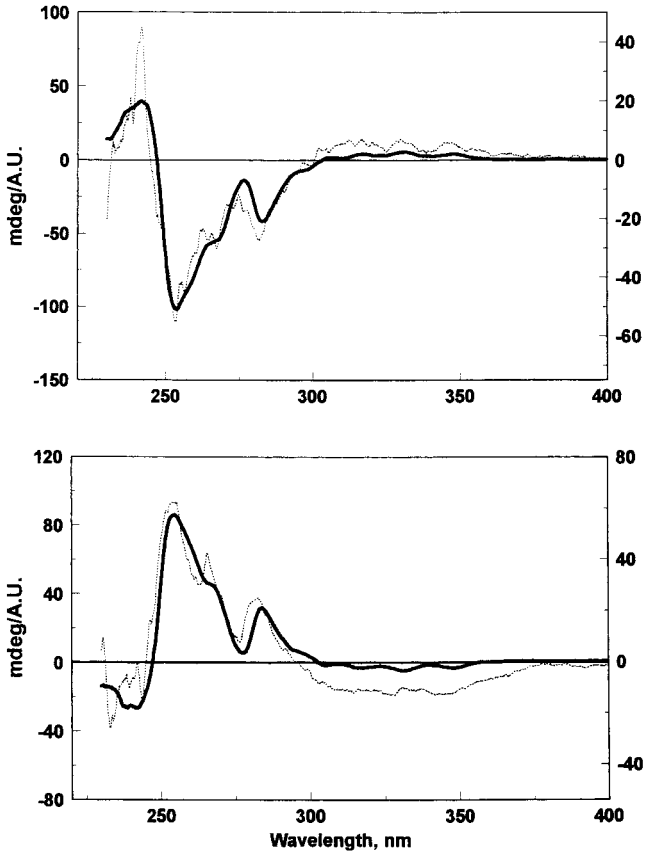

FIGURE 3: CD spectra of 10*R*-(+)-*cis*- (top) and 10*S*-(−)-*cis*-*anti*-BPDE-N^2-dG (bottom) mononucleoside adducts. Dotted lines: Mononucleoside adducts from enzyme digests of BPDE-modified oligodeoxynucleotides. Solid lines: (+)- and (−)-*cis*-*anti*-BPDE-N^2-dG mononucleoside adduct standards.

in good agreement with those of the two adduct standards (heavy lines), thus establishing the stereochemistry of these adducts.

Sites of modification at G_1 or G_2 were determined by the Maxam−Gilbert method; results are summarized in the gel autoradiograph shown in Figure 4. Individual oligonucleotide samples are labeled G_1(+c), G_2(+c), G_1(−c), and G_2-(−c) to denote oligonucleotide sequences with (+)-*cis*- or (−)-*cis*-*anti*-BPDE-N^2-dG lesions at G_1 or G_2. Besides the main intense bands indicated (A, B, and the arrows in Figure 4), other less pronounced bands are also evident. These secondary bands are not present in the untreated oligonucleotides (lanes G_1 and G_2) and are due to nonspecific Maxam−Gilbert reactions at sites other than G that occur with finite probabilities.

Transformation of E. coli. Table 1 records the number of transformants obtained with each construct in the presence or absence of induced SOS functions. Since large fractions of transformants obtained in the absence of SOS induction contained progeny plasmid derived from the parental pMS2 vector, the numbers of transformants (Table 1) were corrected for those having the sequence of the ligated oligonucleotide. Regardless of their position, (−)-cis adducts strongly reduced the yield of transformants recovered from noninduced cells. The G_2(+)-cis adduct also decreased the number of transformants strongly, but with a stereochemically identical adduct positioned at G_1, the fraction of transformants recovered is 16 times higher. This result with (+)-cis adduct was reproducible. The reduced numbers of transformants, probably due to the inhibitory effects on DNA synthesis, were increased following induction of SOS function; relative survival increased 7−38-fold, depending on the position and stereochemical configuration of the adducts. The reduction of the number of transformants by the two stereoisomeric adducts was similar except at G_1, where the (−)-cis adduct was 7 times more inhibitory than the (+)-cis adduct.

Mutagenic Potential of (+) and (−)-cis-anti-BPDE-N^2-dG Adducts. Results of mutagenesis experiments with the (+)- and (−)-*cis*-*anti*-BPDE-N^2-dG adducts, G_1(+c), G_2(+c), G_1(−c), and G_2(−c) are summarized in Table 2. Mutation frequencies for each specificity are arranged as bar graphs in Figures 5 and 6, along with previously acquired data for the stereoisomeric (+) and (−)-*trans*-*anti*-BPDE-N^2-dG adducts, G_1(+t), G_2(+t), G_1(−t), and G_2(−t) (*29*).

In *E. coli*, targeted mutation frequencies for the two cis adducts, studied in two different sequence contexts in the presence of SOS induction, varied from less than 1.3−40%. In the absence of SOS induction, mutational analysis was very limited for the modified constructs except G_1(+c) due to the low yield of transformants, and the results were not included in Table 2. Lowest and highest values were observed for the (+)-cis adduct located at G_2 and the (−)-cis adduct at G_1, respectively. G → T transversions predominated at G_1 and G_2 for both stereoisomeric adducts, but some G → A and a few G → C mutations also were observed. The (−)-cis adduct was significantly more mutagenic than the (+)-cis adduct at both G_1 and G_2. The mutation frequency was higher at G_1 than at G_2 for both adducts.

In COS cells, mutation frequencies ranged from 5 to 12%, and the effects of absolute configuration and adduct position are less marked than in *E. coli*. Mutation frequencies for both adducts were somewhat higher at G_2 than at G_1. Mutational specificity is similar to that observed in *E. coli* with G → T transversions predominating; furthermore, lesser amounts of G → A transitions and G → C transversions also were observed. The (+)- and (−)-cis stereoisomeric adducts were comparably mutagenic at the G_1 and G_2 sites.

DISCUSSION

Comparisons of Mutagenic Effects Induced by cis- and trans-anti-BPDE-N^2-dG Adducts. The two stereoisomeric 10*R*-(+)-*cis*- and 10*R*-(−)-*trans*-*anti*-BPDE-N^2-dG adducts have the same absolute 10*R* configuration at the BPDE-C10-N^2-dG linkage site (Figure 1). Similarly, the 10*S*-(−)-*cis*- and 10*S*-(+)-*trans*-*anti*-BPDE-N^2-dG adducts have the opposite absolute 10*S* configuration at the BPDE-C10-N^2-dG linkage site. Each 10*R* and 10*S* adduct pair differs by virtue of a mirror image relationship between the three OH substituents at the chiral C7, C8, and C9 carbon atoms of BPDE (Figure 1).

We have previously studied the mutagenic potential of (+)- and (−)-*trans*-*anti*-BPDE-N^2-dG adducts (*29*) under conditions similar to those reported in this paper. Mutational frequencies and specificities of the four stereoisomeric *anti*-BPDE-N^2-dG adducts are compared in Figures 5 and 6.

In COS cells, the two trans adducts are more mutagenic than the two cis adducts. The 10*S*-(+)-trans adduct at G_2 exhibits the highest mutation frequency, giving rise pre-

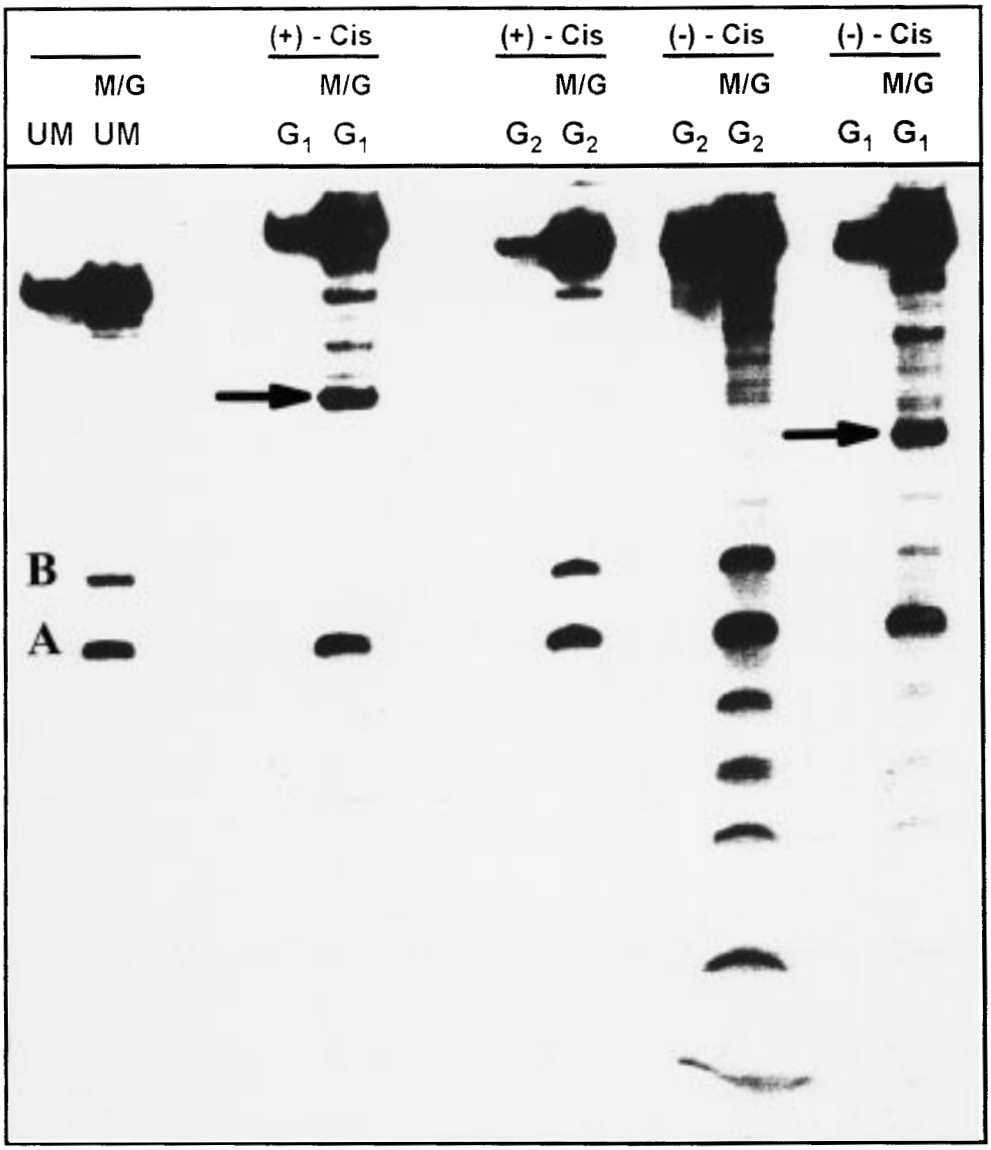

FIGURE 4: Autoradiograph of Maxam−Gilbert (M/G) sequencing gel. UM: unmodified oligonucleotide **I**. G_1 and G_2 denote oligonucleotide sequence **I** with the BPDE residue positioned at the two indicated deoxyguanosines, respectively. The lanes labeled UM, G_1, G_2 show single bands due to the intact oligonucleotide **I**. The lanes labeled M/G contain fragments resulting from Maxam−Gilbert "G" reaction that causes cleavage at deoxyguanosine residues G_1 or G_2 in sequence **I**. The lane "M/G UM" shows bands due to the intact sequence **I** and the two fragments 5′−d(TCCTCCT) (A) and 5-d(TCCTCCTG) (B). In the two lanes labeled "M/G G_1", the highest-mobility band (lowest) exhibits the same mobility as the fragment A in lane "M/G UM"; therefore, this band is identified as fragment A. Lower-mobility G-cleavage fragments are observed in each of these two lanes (arrows) for the (+)-cis and (−)-cis adducts, and are attributed to BPDE-modified fragments B because their mobilities are lower than the mobility of B; the BPDE residue is thus positioned at the site G_1 in these two oligonucleotides. In the lanes labeled "M/G G_2", the two fragments have the same mobilities as the unmodified fragments A and B in lane "M/G UM"; therefore, the BPDE residue is positioned at the site G_2 in these (+)-cis and (−)-cis oligonucleotide adducts.

Table 1: Transformation of *E. coli* AB1157 with DNA Constructs

construct	SOS induction	no. of transformants[a]/50 ng of construct (%)
control	−	13788 (100)
	+	6548 (100)
$G_1(+c)$	−	2808 (20)
	+	9191 (140)
$G_2(+c)$	−	181 (1)
	+	2458 (38)
$G_1(-c)$	−	370 (3)
	+	3097 (47)
$G_2(-c)$	−	482 (4)
	+	1800 (28)

[a] Numbers are corrected for those with a 15-mer insert.

dominantly to G → T transversions at that site. Figure 6 clearly shows that the 10*R* or 10*S* absolute adduct configuration alone is not a major determinant of mutational frequency or specificity. For example, the G → T mutation frequencies are comparable for the 10*S*-(+)-trans- and the 10*R*-(−)-trans adducts at G_1, while at G_2, the 10*S*-(−)-*cis*- and 10*R*-(+)-*cis*-*anti*-BPDE-N^2-dG adducts also exhibit similar G → T mutation frequencies. The exceptionally high mutagenicity of the 10*S*-(+)-trans adduct at G_2 thus is associated with 10*S* stereochemistry as well as the absolute configurations of the OH groups in the BPDE residue. With the exception of the (+)-trans adduct at G_2, mammalian DNA polymerases in COS cells are not particularly sensitive to the stereochemical characteristics of the *anti*-BPDE-N^2-dG lesions. However, a base-sequence effect is observed since there is a greater number of G → A transitions and G → C

Table 2: Mutagenicity of (+) or (−)-*cis*-Bpde-N^2-dG

		no. of targeted events (BPDE-dG → G, T, A, or C)					
construct	host	G	T	A	C	untargeted mutations	targeted mutation frequency[a] (%)
G_1(+*c*)	AB1157UV[b]	62 (77)[c]	15 (19)	2 (2)	2 (2)		23
	COS7	142 (94)	6 (4)	2 (1)		1[d](1)	5
G_2(+*c*)	AB1157UV	76 (100)					<1.3
	COS7	120 (87)	13 (9)	3 (2)		2[e](1)	12
G_1(−*c*)	AB1157UV	43 (60)	24 (33)	4 (6)	1 (1)		40
	COS7	194 (92)	15 (7)	1 (0.5)		1[f](0.5)	8
G_2(−*c*)	AB1157UV	57 (85)	7 (10)	3 (5)			15
	COS7	159 (85)	17 (9)	4 (2)		7[g](4)	11

[a] The total number of targeted mutants divided by the effective number of transformants analyzed. Progeny derived from scaffold was omitted from this calculation. [b] SOS-induced AB1157. [c] Percentage. [d] TCCTCtTGGCCTCTC. [e] TaCTCCTGGCCTCTC and aCCTtCTGGCCTCTC. [f] TaCTC-CTGGCCTCTC. [g] Four mutants with TtCTCCTGGCCTCTC and one mutant each with TCtTCCTGGCCTCTC, TtCTtCTGGCCTCTC, or TtCTCCgGGCCTCTC (mutations are shown in lowercase).

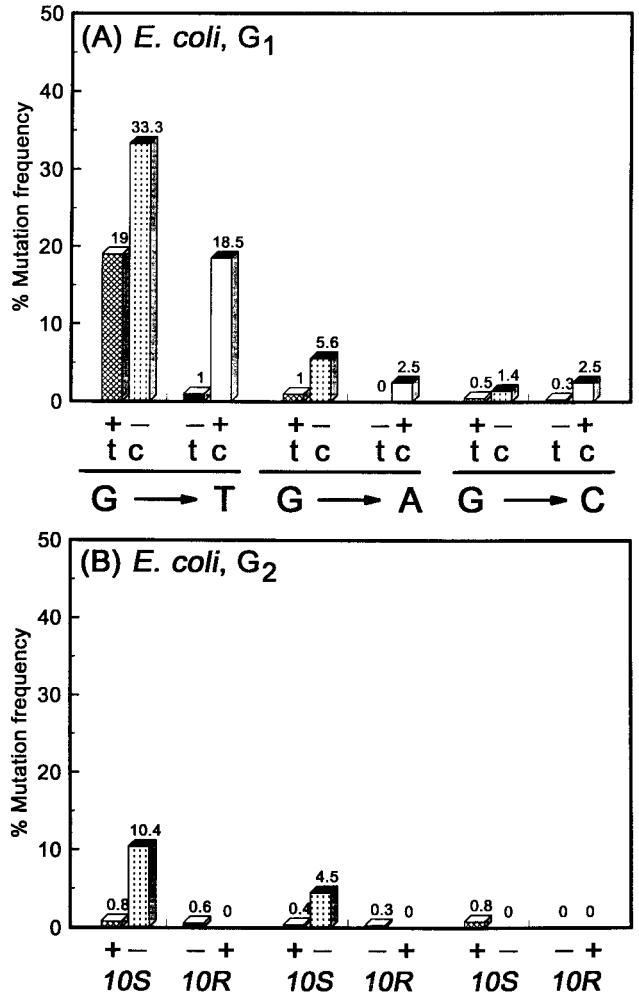

FIGURE 5: Frequencies of G → T, G → A, and G → C mutations (expressed as a percentage of all replication events that result in no mutation, or targeted base substitution mutations) induced by stereoisomeric *anti*-BPDE-N^2-dG at positions G_1 or G_2 in sequence **I** in SOS-induced *E. coli*. The plus and minus signs refer to adducts generated from (+)- or (−)-*anti*-BPDE, respectively, while t and c refer to trans and cis adduct stereochemistry at the linkage site (Figure 1); the absolute configurations (10*S* or 10*R*) are indicated at the bottom.

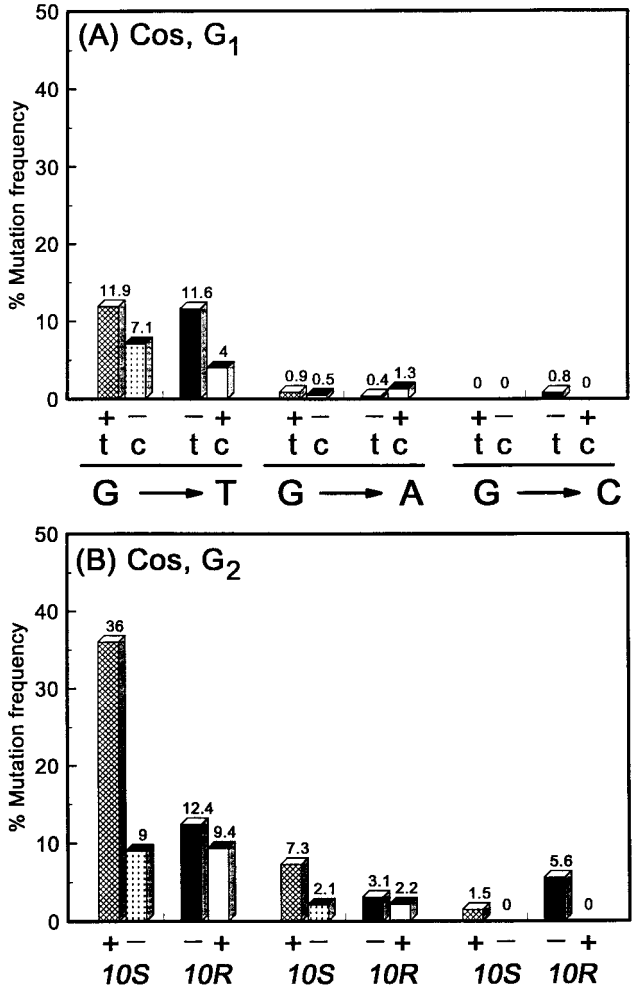

FIGURE 6: Frequencies of G → T, G → A, and G → C mutations (expressed as a percentage of all replication events that result in no mutation, or targeted base substitution mutations) induced by stereoisomeric *anti*-BPDE-N^2-dG at positions G_1 or G_2 in sequence **I** in COS cells. All other symbols and designations as in Figure 5.

transversions at G_2 (GG_2C) than at G_1 (TG_1G sequence context).

In contrast to the somewhat greater mutation frequencies of the two trans adducts relative to the two cis adducts in COS cells, the two cis adducts are clearly more mutagenic in *E. coli* than their trans adduct counterparts (Figure 5). Among the trans adducts, the 10*S*-(+)-*trans*-*anti*-BPDE-N^2-dG adduct is highly mutagenic only at G_1, generating G → T transversions. The 10*R*-(+)-cis adduct generates an equal frequency of G → T transversions at the same site. Thus, differences in the 10*R* and 10*S* absolute configurations at the adduct linkage site do not significantly affect G → T mutation frequencies at G_1. On the other hand, frequencies of G → T transversions at G_1 are more than 30 times greater for the 10*S*-(−)-cis adduct than for the 10*R*-(−)-trans adduct

(Figure 5); configurations of the OH substituents are identical in the two adducts that differ only in the opposite orientations of the dG residues about the chiral C10 carbon center. At G_2, only the (−)-cis adduct gives rise to significant number of G → T and G → A mutations. Overall, the effects of adduct stereochemistry and position are much more strongly pronounced in *E. coli* than in COS cells.

It is evident from this work and our previous study (*29*) that in any given host, mutational events are influenced by adduct stereochemistry and sequence context. Our results also indicate that the mutagenic potentials of stereochemically identical *anti*-BPDE-N^2-dG lesions embedded in the same sequence context depend markedly on the DNA polymerase involved. This suggests that the interaction between the (stereochemically defined) *anti*-BPDE-N^2-dG adduct and DNA polymerase is not uniform, leading to the differences in mutation frequencies observed in *E. coli* and COS cells.

BPDE Reactivity, DNA Repair, and Mutation Hot Spots. It is recognized that certain bases in DNA undergo mutations much more frequently than the same bases in other sequence contexts, giving rise to characteristic "fingerprints" for specific carcinogens (*11*, *42*). Several factors may contribute to mutational hotspot phenomena including reactivity hotspots, sequence-dependent error-prone polymerase bypass, and sequence-dependent excision of adducts by repair enzymes. In our model system, the single-stranded vector minimizes DNA repair (*36*).

The cis adducts are more mutagenic than trans adducts in *E. coli*; overall, they are only somewhat less mutagenic than the trans adducts in COS cells (Figures 5 and 6). It is clear that contributions of the less abundant cis adducts to the overall mutagenic burden of *anti*-BPDE should not be neglected. Differential rates of DNA excision repair may play a particularly important role. Zou et al. (*43*) found that *cis-anti*-BPDE-N^2-dG lesions are excised in vitro by the *E. coli* Uvr(A)BC exinuclease system in a 5′CG*C sequence context (the asterisk indicates the modified dG residue) at a rate 2−3 times faster than the *trans-anti*-BPDE-N^2-dG adducts. Human DNA repair enzyme complexes excise the two cis adducts from the same 5′CG*C sequence context at rates 10 times faster than the stereoisomeric trans adducts (*44*). If similar differences exist in other sequence contexts, then the mutagenic burden of cis adducts in vivo should be significantly lower than that of the *trans-anti*-BPDE-N^2-dG adducts.

Effects of Adduct Conformation. With the (+)-*trans-anti*-BPDE-N^2-dG lesion positioned at a single strand-double strand junction (ss/ds), but without a partner base opposite the modified dG residue in the growing DNA strand, the bulky hydrophobic BPDE residue stacks with the terminal base on the complementary strand (*45*). In this conformation, the BPDE residue fills space normally occupied by the aromatic portion of the 2′-deoxynucleotide triphosphate (dNTP) in the DNA ss/ds junction-polymerase replication complex. Since the dNTP residue is prevented from forming normal hydrogen bonds with the modified dG residue, the BPDE residues constitute a strong block to DNA synthesis. For DNA synthesis to occur, the BPDE residue must swing away from its carcinogen-base stacked position (*44*) and allow insertion of a dNTP opposite the modified dG. Polymerase bypass of these bulky lesions implies that some sequence-dependent flexibility must exist at these junctions to allow for error-prone or correct bypass of the lesion. No doubt, the conformational details and the dynamics of the conformational flexibility depend on the stereochemical properties of the lesions and probably also in the base sequence context in which the lesions are embedded. Elucidation of these complex factors, particularly in the presence of different polymerases, remains a challenging and formidable task. Nevertheless, it is clear that these interdependent parameters determine translesional events across BPDE-DNA adducts in different sequence contexts.

With the addition of the partner base dC at the end of the growing strand opposite the (+)-*trans-anti*-BPDE-N^2-dG adduct, the bulky BPDE residue no longer stacks with the terminal bases on the growing DNA strand (*46*) and assumes a conformation similar to the minor groove structure observed in double-stranded DNA (*47*). In this orientation, the BPDE residue should interfere less strongly with the insertion of the next dNTP residue opposite the flanking base on the 5′ side of the BPDE-modified dG on the template strand. However, because the normal conformation of the ss/ds junction is compromised by the presence of the bulky BPDE residue, the rate of DNA synthesis should still be slowed.

Comparison with Other Site-Specific Mutagenesis Studies. When the *supF* gene in pUB3 was treated with (+)-*anti*-BPDE and subsequently introduced into *E. coli*, hot spots of mutations most frequently were detected at tandem GG sequences. A strong hot spot of mutation was found at G_{115} in the sequence context 5′GCG$_{115}$G$_{116}$CCAAAG (**II**), while few mutations were observed at G_{116} (*22*). Interestingly, mutational hot spots in runs of two guanines, 5′- - -GG- - - - were also observed at the HPRT locus in V-79 cells (*9*, *23*), but the highest mutation frequencies were found at the 3′-G rather than the 5′-G. These findings are consistent with our studies of the (+)-*trans*- and (+)-*cis-anti*-BPDE-N^2-dG adducts, both being produced by the reaction of dG with (+)-*anti*-BPDE. In *E. coli*, adducts at G_1 are more mutation prone than at G_2, whereas in COS cells, the mutation frequency is higher at G_2 than at G_1.

In site-specific mutagenesis experiments with (+)-*trans-anti*-BPDE-N^2-dG adducts in *E. coli* (ES87), G → T transversions were observed almost exclusively in the sequence context 5′TGC (*27*). In other studies with the same adduct at G_{115} in sequence **II** in *E. coli*, the dominant mutations were G → T transversions accompanied by smaller numbers of G → A and G → C mutations (*28*); with the same adduct at G_{116}, the overall mutation frequency was ∼8 times lower, but the mutational specificity was similar. Hanrahan et al. (*30*) studied the replication of the (+)-*trans-anti*-BPDE-N^2-dG adducts at G_{115} and G_{116} in sequence **II** using an M13 DNA vector in *E. coli* (DL7); following replication in SOS-induced cells, 40% base substitutions (mainly G → T) occurred at G_{115} and only 12% at G_{116}. These results are in qualitative agreement with our *E. coli* (AB1157) site-specific mutagenesis experiments in the sequence context 5′TG$_1$G$_2$C (Figure 5). However, there are some differences: the ratio of G_1/G_2 mutation frequency (G → T) was >20 in our case, and the fractions of G → A and G → C mutations were smaller than those reported by Jelinsky et al. (*28*) and Hanrahan et al. (*30*). The relatively small differences could be associated with differences in sequence context or the different *E. coli* strains.

The mutation frequencies of the (+)-*trans*-, (−)-*trans*-, (+)-*cis*-, and (−)-*cis*-*anti*-BPDE-N^2-dG in a $^{5'}CG_{144}T$ sequence context of the *sup*F gene was studied by Shukla et al. (*31*, *32*). While G → T transversions dominate in sequence contexts $^{5'}$TG*C (*27*), $^{5'}$CG*G and $^{5'}$GG*C (*28*, *30*), $^{5'}$TG*G and $^{5'}$GG*C (*29*, and this work), G → A transitions dominate in the case of the 10*S*-(+)-trans- and (−)-cis adducts with much smaller amounts of G → T and G → C base substitutions observed in the $^{5'}CG_{144}T$ sequence context (*32*). In the case of the 10*R*-(−)-*trans*- and (+)-*cis*-*anti*-BPDE-N^2-dG adducts, nearly comparable numbers of G → T, G → A, and G → C mutations were observed. One major difference between these results and ours, in addition to mutational specificity (Figure 5), is that (−)-trans adducts are practically nonmutagenic in our sequence context in *E. coli*. Furthermore, the 10*R*-(+)-cis and 10*S*-(−)-cis adducts are much more mutagenic than the two trans adducts (Figure 5); thus, the *R* and *S* grouping of the mutational frequency and specificity observed by Shukla et al. (*32*) does not prevail in the TG*G and GG*C sequence contexts in our *E. coli* system.

This study clearly indicates that base sequence effects and adduct stereochemistry play critical roles in site-specific mutagenesis experiments in *E. coli.* Site-specific mutagenesis studies with *anti*-BPDE-N^2-dG adducts in mammalian cells (*29*, this work) show that, with the exception of the unusually high mutation frequency (G → T) of the (+)-*trans*-*anti*-BPDE-N^2-dG adduct at G_2 (Figure 6), the effects of adduct stereochemistry appear to be less important in COS cells than in *E. coli*.

SUMMARY AND CONCLUSION

In any given host, mutagenic events induced by *anti*-BPDE-N^2-dG adducts are influenced by the bases flanking the lesions. Interactions between the *anti*-BPDE-N^2-dG adducts of a particular conformation and various DNA polymerases are not uniform, leading to differences in mutational events in *E. coli* and in mammalian (COS) cells. These effects may reflect differences in the structures of the replication complex. On the basis of our studies and those of others, we conclude that the fidelity of translesional synthesis past *anti*-BPDE-N^2-dG adducts is determined by a complex interplay between DNA adduct stereochemistry, flanking bases and properties of the DNA replication complex.

ACKNOWLEDGMENT

The authors thank Ms. Susan Rigby for assistance in preparing the manuscript.

REFERENCES

1. Conney, A. H. (1982) *Cancer Res. 42*, 4875−4917.
2. Singer, B., and Grunberger, D. (1983) *Molecular Biology of Mutagens and Carcinogens*, Plenum Press, New York.
3. Phillips, D. H. (1983) *Nature 303*, 468−472.
4. Buening, M. K., Wislocki, P. G., Levin, W., Yagi, H., Thakker, D. R., Akagi, H., Koreeda, M., Jerina, D. M., and Conney, A. H. (1978) *Proc. Natl. Acad. Sci. U.S.A. 75*, 5358−5361.
5. Slaga, T. J., Bracken, W. J., Gleason, G., Levin, W., Yagi, H., Jerina, D. M., and Conney, A. H. (1979) *Cancer Res. 39*, 67−71.
6. Wood, A. W., Chang, R. L., Levin, W., Yagi, H., Thakker, D. R., Jerina, D. M., and Conney, A. H. (1977) *Biochem. Biophys. Res. Commun. 77*, 1389−1396.
7. Brookes, P., and Osborne, M. R. (1982) *Carcinogenesis 3*, 1223−1226.
8. Stevens, C. W., Bouck, N., Burgess, J. A., and Fahl, W. E. (1985) *Mutat. Res. 152*, 5−14.
9. Wei, S.-J. C., Chang, R. L., Hennig, E., Cui, X. X., Merkler, K. A., Wong, C.-Q., Yagi, H., and Conney, A. H. (1994) *Carcinogenesis 15*, 1729−1735.
10. Ross, J. A., Nelson, G. B., Wilson, K. H., Rabinowitz, J. R., Galati, A., Stoner, G. D., Nesnow, S., and Mass, M. J. (1995) *Cancer Res. 55*, 1039−1044.
11. Denissenko, M. F., Pao, A., Tang, M.-S., and Pfeifer, G. (1996) *Science 274*, 430−432.
12. Weinstein, I. B., Jeffrey, A. M., Jennette, K. W., Blobstein, S. H., Harvey, R. G., Harris, C., Autrup, H., Kasai, H., and Nakanishi, K. (1976) *Science 193*, 592−594.
13. Koreeda, M., Moore, P. D., Wislocki, P. G., Levin, W., Conney, A. H., Yagi, H., and Jerina, D. M. (1978) *Science 199*, 778−781.
14. Meehan, T., and Straub, K. (1979) *Nature 277*, 410−412.
15. Cheng, S. C., Hilton, B. D., Roman, J. M., and Dipple, A. (1989) *Chem. Res. Toxicol. 2*, 334−340.
16. Bernelot-Moens, C., Glickman, B. W., and Gordon, A. J. E. (1990) *Carcinogenesis 11*, 781−785.
17. Eisenstadt, E., Warren, A. J., Porter, J., Atkins, D., and Miller, J. H. (1982) *Proc. Natl. Acad. Sci. U.S.A. 79*, 1945−1949.
18. Mazur, M., and Glickman, B. W. (1988) *Somat. Cell. Mol. Genet. 14*, 393−400.
19. Carothers, A. M., and Grunberger, D. (1990) *Carcinogenesis 11*, 189−192.
20. Keohavong, P., and Thilly, W. G. (1992) *Proc. Natl. Acad. Sci. U.S.A. 89*, 4623−4627.
21. Yang, J.-L, Maher, V. M., and McCormick, J. J. (1987) *Proc. Natl. Acad. Sci. U.S.A. 84*, 3787−3791.
22. Rodriguez, H., and Loechler, E. L. (1993) *Carcinogenesis 14*, 373−383.
23. Wei, S. J. C., Chang, R. L., Bachech, N., Cui, X. X., Merkler, K. A., Wong, C. Q., Hennig, E., Yagi, H., Jerina, D. M., and Conney, A. H. (1993) *Cancer Res. 53*, 3294−3301.
24. Basu, A. K., and Essigman, J. M. (1988) *Chem. Res. Toxicol. 1*, 1−18.
25. Singer, B., and Essigman, J. M. (1991) *Carcinogenesis 12*, 949−955.
26. Loechler, E. L. (1996) *Carcinogenesis 17*, 895−902.
27. Mackay, W., Benasutti, M., Drouin, E., and Loechler, E. L. (1992) *Carcinogenesis 13*, 1415−1425.
28. Jelinsky, S. A., Liu, T., Geacintov, N. E., and Loechler, E. L. (1995) *Biochemistry 34*, 13545−13553.
29. Moriya, M., Spiegel, S., Fernandes, A., Amin, S., Liu, T., Geacintov, N., and Grollman, A. P. (1996) *Biochemistry 35*, 16646−16651.
30. Hanrahan, C. J., Bacolod, M. D., Vyas, R. R., Liu, T., Geacintov, N. E., Loechler, E. L., and Basu, A. K. (1997) *Chem. Res. Toxicol. 10*, 369−377.
31. Shukla, R., Liu, T., Geacintov, N. E., and Loechler, E. L. (1997) *Biochemistry 36*, 10256−10261.
32. Shukla, R., Jelinsky, S., Liu, T., Geacintov, N. E., and Loechler, E. L. (1997) *Biochemistry 36*, 13263−13269.
33. Chary, P., Latham, G. J., Robberson, D. L., Kim, S. J., Han, S., Harris, C. M., Harris, T. M., and Lloyd, R. S. (1995) *J. Biol. Chem. 270*, 4990−5000.
34. Liu, T., Xu, J., Tsao, H., Li, B., Xu, R., Yang, C., Moryia, M., and Geacintov, N. E. (1995) *Chem. Res. Toxicol. 9*, 255−261.
35. Yagi, H., Thakker, D. R., Hernandez, O., Koreeda, M., and Jerina, D. M. (1977) *J. Am. Chem. Soc., 99*, 1604−1611.
36. Moriya, M. (1993) *Proc. Natl. Acad. Sci. U.S.A. 90*, 1122−1126.
37. Moriya, M., Zhang, W., Johnson, F., and Grollman, A. P. (1994) *Proc. Natl. Acad. Sci. U.S.A. 91*, 11899−11903.
38. Pandya, G. A., and Moriya, M. (1996) *Biochemistry 35*, 11487−11492.

39. Hirt, B. (1967) *J. Mol. Biol. 26*, 365−369.
40. Chung, C. T., Niemala, S. L., and Miller, R. H. (1989) *Proc. Natl. Acad. Sci. U.S.A. 86*, 2172−2175.
41. Moriya, M., and Grollman, A. P. (1993) *Mol. Gen. Genet. 239*, 72−76.
42. Vogelstein, B., and Kinzler, K. W. (1992) *Nature 355*, 209−210.
43. Zou, Y., Liu, T., Geacintov, N. E., and Van Houten, B. (1995) *Biochemistry 34*, 13582−13593.
44. Hess, M. T., Gunz, D., Luneva, N., and Geacintov, N. E. (1998) *Mol. Cell. Biol.* (In press).
45. Cosman, M., Hingerty, B., Geacintov, N. E., Broyde, S., and Patel, D. J. (1995) *Biochemistry 34*, 15334−1550.
46. Feng, B., Gorin, A., Hingerty, B. E., Geacintov, N. E., Broyde, S., and Patel, D. J. (1997) *Biochemistry 36*, 13769−13779.
47. Cosman, M., de los Santos, C., Fiala, R., Hingerty, B. E., Singh, S., Ibanez, V., Margulis, L. A., Live, D., Geacintov, N. E., Broyde, S., and Patel, D. J. (1992) *Proc. Natl. Acad. Sci. U.S.A. 89*, 1914−1918.

BI980401F